Hardware Emulations

using 5G Toolkit and SDRs: Hands-on

For academia only

Contributors:

Editor:	Simulator Design Team, GIGAYASA
Contributing Authors:	Aman Mishra, Vijaya Mareedu and Vikram Singh, GIGAYASA

Grants and Funding

Gigayasa is supported by:

- Indian Institute of Technology, Madras Incubation Center (IITM-IC).
- Startup India.
- Department of Telecommunication (DoT), India.
- Center of Excellence in Wireless Technology (CEWiT), IITM.
- Ministry of Electronics and Information Technology (MEITy), India.

Contents

1 | Implementation of OFDM in 5G networks

Orthogonal Frequency Division Multiplexing (OFDM) is a modulation technique used in wireless communication systems to transmit data over radio waves. It works by dividing the available spectrum into multiple orthogonal (non-overlapping) subcarriers, each carrying one constellation symbol. These subcarriers are spaced apart at precise intervals, ensuring they do not interfere with each other. OFDM is widely used in various wireless communication standards such as Wi-Fi, LTE (Long-Term Evolution), WiMAX, and 5G due to its ability to provide high-speed data transmission, robustness to interference, and efficient spectrum utilization. In this chapter, we will discuss the design of OFDM used in the air interface of the 5G networks.

1.1 | Introduction to Multiplexing Schemes

Every generation of cellular networks used a suitable waveform to support multiple access and manage time, frequency, and inter-node interference. The first (1^{st}) and second (2^{nd}) generations of cellular networks used **f**requency **d**ivision **m**ultiplexing (FDD) to allocate resources to multiple user equipments (UEs) in the uplink (UL) and downlink (DL). However, FDD resulted in under-utilization of system bandwidth due to wastage resulting from the guard band. The guard band in FDD is necessary to counter the radiation leaking from the signal transmission in adjacent channels. These losses were reduced in the third (3^{rd}) generation of cellular networks by using **t**ime **d**ivision **d**uplexing (TDD) and **c**ode **d**ivision **m**ultiple **a**ccess (CDMA) based telephony. The fourth (4^{th}) generation of wireless networks was designed to support mobile phone-based internet and many new use-cases using 20 MHz of bandwidth. The high sample rate resulted in highly frequency-selective channels, demanding complex time-domain receivers. These receivers were power-hungry and required large silicon footprints. This challenge was addressed by OFDM technology, which was a low complexity implementation of multi-carrier modulation (MCM) schemes enabled by FFT algorithms, which can be implemented very efficiently on hardware accelerators.

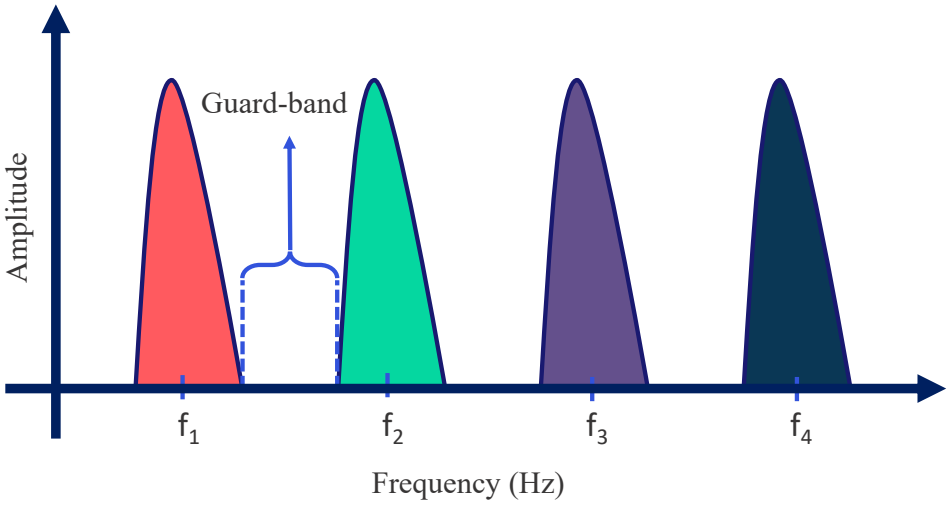

Figure 1.1: Frequency division multiplexing (FDM)

1.1.1 | Multi-Carrier Modulation (MCM)

The MCM transmits information symbols $s_k[n]$ using multiple carriers of frequency (f_k) defined by,

$$m_k(t) = s_k[n].cos(2\pi f_k t) \tag{1.1}$$

where $f_k = \frac{k}{T}$ is the k^{th} harmonic for the fundamental frequency transmitted in the n^{th} symbol period $t \in [nT, (n+1)T]$. The N carriers can be used to transmit N constellation symbols in a period of T seconds.. The symbols are loaded onto each carrier and all the carriers are superimposed to form a

multi-carrier modulated (MCM) signal,

$$m(t) = \sum_{k=0}^{N-1} m_k(t) \tag{1.2}$$

$$= \sum_{k=0}^{N-1} s_k[n].cos(2\pi f_k t) \tag{1.3}$$

This MCM signal is up-converted to the carrier frequency f_c before transmission,

$$x(t) = m(t).cos(\omega_c t) \tag{1.4}$$

as shown in figure 1.2. This signal has spans a pass-band bandwidth of $\frac{N}{T}$ and transmits $\frac{Q_m.N}{T}$ bits per second where Q_m defines the number of bits per constellation (QAM/PSK) symbols. The Q_m is also known as modulation order in 5G networks.

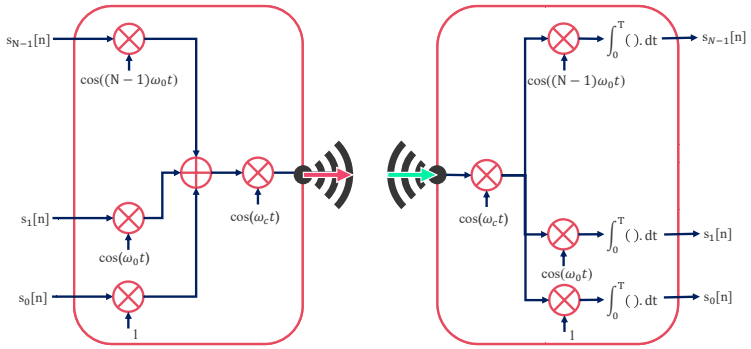

Figure 1.2: Transmitter and Receiver Design for multi-carrier modulations

Owing to the orthogonality property[2], of sinusoids defined by,

$$\int_{nT}^{(n+1)T} 2.cos(2\pi f_j t).cos(2\pi f_k t)dt = \begin{cases} 1, & j = k \\ 0, & j \neq k \end{cases} \tag{1.5}$$

the transmitted information symbols can be decoded easily at the receiver. The process of multiplying the carrier tone with the down-converted signal $r(t)$ and integrating it over a period T is called correlation. Each symbol is decoded using a correlator,

$$\hat{s}_k[n] = \int_{nT}^{(n+1)T} 2.r(t).cos(2\pi f_k t)dt \tag{1.6}$$

The multi-carrier modulation schemes have the ability to divide the entire carrier bandwidth into multiple subcarriers, where each subcarrier can carry information that can be decoded independently at the receiver. The property that makes MCM particularly suitable for wideband communication is the simplicity in demodulation. The multi-path channel is modelled as,

$$h(t,\tau) = \sum_{l=0}^{l=L-1} \alpha_l.\delta(t - \tau_l) \tag{1.7}$$

This equation of wireless channel results in a system model defined by,

$$y(t) = x(t) \otimes h(t,\tau) \tag{1.8}$$

$$= x(t) \otimes \sum_{l=0}^{L-1} \alpha_l.\delta(t - \tau_l) \tag{1.9}$$

$$= \sum_{l=0}^{L-1} \alpha_l.x(t - \tau_l) \tag{1.10}$$

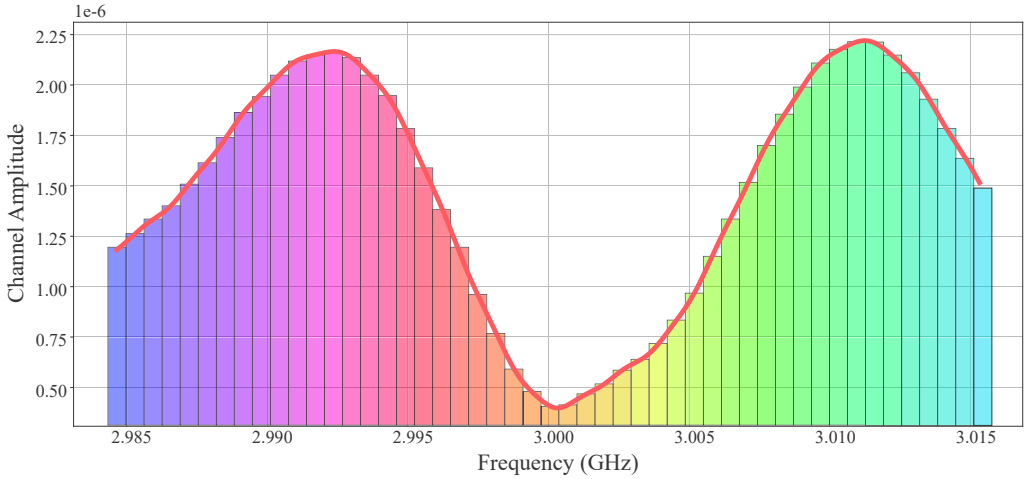

Figure 1.3: Frequency Selectivity in channel due to multipath propagation

where $\otimes$ is the convolution operator and $x(t)$ is the pass-band transmitted signal. The base-band representation of this received signal is given by

$$r(t) = \sum_{l=0}^{L-1} \alpha_l . m(t - \tau_l) \tag{1.11}$$

This signal when passed through the k^{th} correlator results in,

$$\begin{aligned}
\hat{r}_k[n] &= \int_{nT}^{(n+1)T} 2.r(t).cos(2\pi f_k t)dt \\
&= \int_{nT}^{(n+1)T} 2.\sum_{l=0}^{L-1} \alpha_l . m(t - \tau_l).cos(2\pi f_k t)dt \\
&= \sum_{l=0}^{L-1} 2.\alpha_l . \int_{nT}^{(n+1)T} m(t - \tau_l).cos(2\pi f_k t)dt \\
&= \sum_{l=0}^{L-1} 2.\alpha_l . \int_{nT}^{(n+1)T} \sum_{k=0}^{N-1} s_k[n].cos(2\pi f_k (t - \tau_l)).cos(2\pi f_k t)dt \\
&= \sum_{l=0}^{L-1} 2.\alpha_l . \sum_{k=0}^{N-1} s_k[n]. \int_{nT}^{(n+1)T} cos(2\pi f_k (t - \tau_l))cos(2\pi f_j t)dt \\
&= \sum_{l=0}^{L-1} 2.\alpha_l . \sum_{k=0}^{N-1} s_k[n].cos(2\pi f_k \tau_l).\delta(k - j) \\
&= \sum_{l=0}^{L-1} \alpha_l . s_k[n].cos(2\pi f_k \tau_l) \\
&= s_k[n]. \sum_{l=0}^{L-1} .\alpha_l .cos(2\pi f_k \tau_l) \qquad (1.12) \\
&= s_k[n].h_k[n] \qquad (1.13)
\end{aligned}$$

The result in equation 1.13 very clearly shows that the multiplicative relation between the transmitted and received signal unlike the correlative relation in time domain. The correlation based relation uses very complex signal processing to cancel the inter-symbol interference to decode the signal accurately at the receiver. These algorithms consumes very high power and requires expensive circuitry in comparison to receivers with multiplicative relation which only requires a division to decode the information. However, its important to note that each correlator consists of one local oscillator and one integrator. Hence transmitting N symbols in time period T requires N oscillator at the the transmitter and N correlators

at the receiver. This results in high complexity, power consumption and cost. Although each subcarrier experiences a flat fading, the wireless channel in frequency domain $H(f) = \sum_{l=0}^{l=L-1} \alpha_l . e^{i.2\pi.f.\tau_l}$ offers different gain and non-linear phase to each of these sub-carriers as shown in figure 1.3. However, this challenge can be addressed using simple channel estimation and interpolation schemes which will be discussed in details in chapter **??**.

1.1.2 | Efficient Implementations of MCM

The major limitations of the the MCM are its high computation complexity and high cost. Both these drawbacks are rooted in modulation and demodulation schemes given by,

$$
\begin{aligned}
\textbf{MCM Modulation} \quad & = \sum_{k=0}^{N-1} s_k[n].cos(2\pi k.\Delta f t) \\
& = \mathcal{R}\left\{\sum_{k=0}^{N-1} s_k[n].e^{2\pi k.\Delta f t}\right\} \\
& = \mathcal{F}^{-1}\left\{s_k\right\} \text{ where } s_k = \left[s_k[0], s_k[1], \ldots, s_k[N-1]\right] \\
\textbf{MCM Demodulation} \quad & = \tfrac{2}{T}\int_{nT}^{(n+1)T} r(t).cos(2\pi f_k t)dt \\
& = \mathcal{R}\left\{\tfrac{2}{T}\int_{nT}^{(n+1)T} r(t).e^{-2\pi k.\Delta f t}dt\right\} \\
& = \mathcal{F}\left\{r(t)\right\}
\end{aligned}
$$

If the modulated and demodulated signal are samples at a rate of $f_s = N.\Delta f$ where $\Delta f = \frac{1}{T}$, the Fourier transform/series can be replaced with Discrete Fourier Transform which can be implemented very efficiently using fast Fourier transform (FFT) algorithms. Furthermore, FFT has very low complexity of the order of $N * log_2(N)$ in comparison MCM and DFT. Both these characteristics helps it overcome the limitations of MCM. However, this implementation suffers from inter-symbol interference due to multi-path propagation resulting in reception of multiple delayed and attenuated copies of the transmitted signal. This problem can be easily addressed by inserting the cyclic prefix to the transmitted signal. The cyclic prefix unlike the zero prefix not only mitigate the inter-symbol interference but also preserve the characteristics of the FFT. This superposition of multiple orthogonal tones, each loaded with information symbol, inserted with cyclic prefix is called orthogonal frequency division multiplexing (OFDM). The OFDM exists in multiple flavours which we will discuss in upcoming sections.

1.2 | Classification of OFDM

As discussed in previous sections, OFDM provides the low complexity receiver implementation of MCM for wideband frequency selective channels. The two most commonly used implementations are

- Cyclic Prefix based OFDM (CP-OFDM) and,
- Discrete Fourier Transform-spread-OFDM (DFT-s-OFDM)

The DFT-s-OFDM is also called as Single Carrier Frequency Division Multiplexing (SC-FDMA). We will discuss both these waveform in details in upcoming sections.

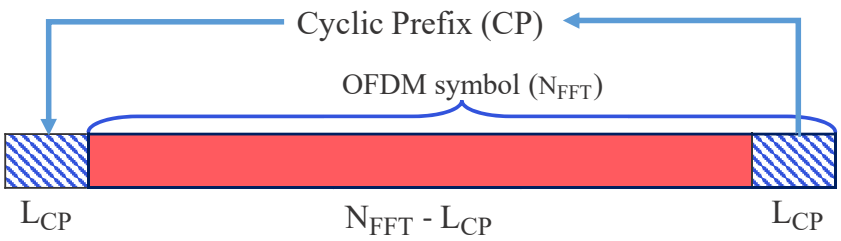

Figure 1.4: Visualization of cyclic prefix (CP)

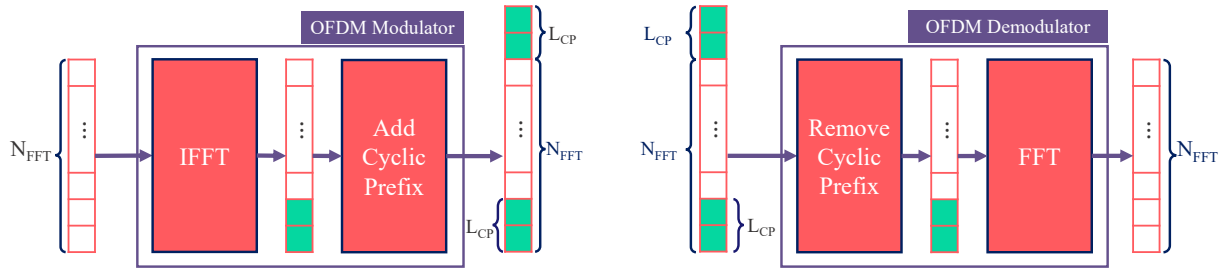

(a) Design of OFDM modulator

(b) Design of OFDM Demodulator

Figure 1.5: Implementation of OFDM

1.2.1 | Cyclic Prefix (CP) based OFDM

The CP-OFDM as discussed in previous section performs two operations:

- Fast Fourier Transform (FFT) to covert the frequency domain block at n-th time instant, $s_n = [s_n[0], s_n[1], \ldots, s_n[N_{FFT} - 1]]$ to time domain samples aka time domain OFDM symbol,
- Attaches CP to time-domain OFDM symbol.

The detailed implementation of OFDM is shown in Fig 1.5a. The FFT helps in converting the convolution between the transmitted samples and the channel to the multiplication which reduces the complexity of decoding the data. The cyclic prefix helps meet two objectives,

- mitigate inter-symbol interference.
- preserve the orthogonality between subcarrier.

The receiver performs complementary operation to transmitter where first CP is removed, followed by the translating the time domain samples to frequency domain block using FFT as shown in Fig 1.5b. This implementation allows for much simple channel estimation and equalization discussed in details **??**.
The OFDM suffers from the problem of low peak to average power ratio (PAPR). The PAPR arises due to constructive interference in the tones in time domain causing the spikes in power for a few time domain samples while the average power stays the same. It limits the radio from transmitting at the maximum transmit power. The large PAPR forces the radio to transmit at much lower power compared to operating point to avoid the amplifier from operating in the non-linear region. The non-linear region causes signal saturation resulting in loss of information.

1.2.2 | DFT-s-OFDM

The cause of high PAPR in OFDM systems is the FFT block, which results in spikes in power due to constructive interference. The effect of PAPR can be reduced by using another DFT of lower order than N_{FFT} to spread the signal. CP-OFDM with DFT as a pre-processing block is called Discrete Fourier Transform-spread-OFDM (DFT-s-OFDM), as shown in Figure 1.6. Spreading by an M_{sc}-point DFT reduces the constructive interference resulting from the de-spreading caused by the FFT block by a factor of M_{sc}. In DFT-s-OFDM, the total number of information/constellation symbols is divided into sets (S), which are computed as follows,

$$\text{Numbers of sets } (S) = \frac{\text{Numbers of information symbols}}{M_{\text{sc}}}. \tag{1.14}$$

The number of sets (S) is equal to the number of OFDM symbols allocated to the respective channel, which is PUSCH or PUCCH for format 3 or format 4 in 5G NR. DFT-s-OFDM supports a single layer transmission and is employed only in the uplink to improve the coverage of the network. It is often used only with $\frac{\pi}{2}-$BPSK modulation when the link-budget is constrained and channel conditions are unfavourable. The illustration of DFT-s-OFDM shown in Fig-1.6 assumes that there is no PTRS transmission along-side the information symbols. The M_{sc} for PUSCH is computed using the expression,

$$M_{\text{sc}}^{\text{PUSCH}} = M_{\text{RB}}^{\text{PUSCH}}.N_{\text{sc}}^{\text{RB}}, \tag{1.15}$$

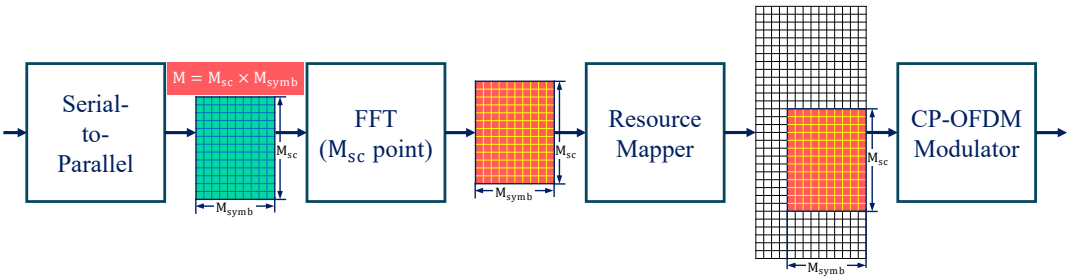

(a) Design of DFT-s-OFDM modulator

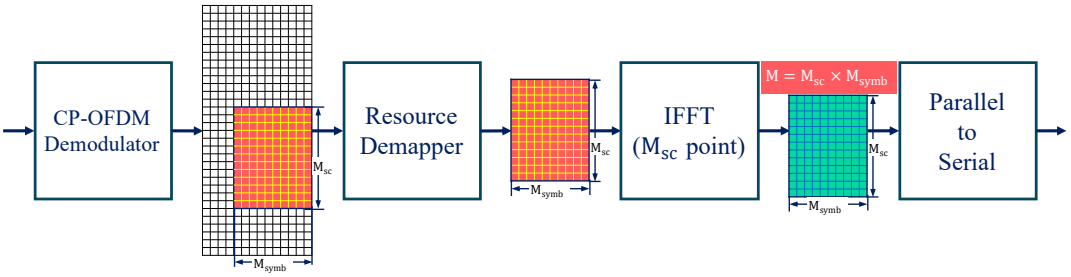

(b) Design of DFT-s-OFDM demodulator

Figure 1.6: Implementation of DFT-s-OFDM

where $N_{\text{sc}}^{\text{RB}} = 12$ and $M_{\text{RB}}^{\text{PUSCH}}$ denotes the RBs allocated to UE for data transmission. This variable in 5G networks is expected to satisfy the condition $M_{\text{RB}}^{\text{PUSCH}} = 2^{\alpha_2}.3^{\alpha_3}.5^{\alpha_5}$ where α_2, α_3, and α_5 are expected be non-negative integers.

1.3 | Why Orthogonal Frequency Division Multiplexing in 5G Networks

OFDM is adopted in 5G NR owing to its ability to cope with severe wideband frequency selective fading conditions and simple implementation. The reasons for the wide spread adoption of OFDM in 5G NR and other wideband communication technologies are listed below.

1. OFDM converts the frequency selective channel to flat fading channel at a subcarrier level, as depicted in Figure-1.3.

   [a] Simplifies the receiver design by converting the wide-band frequency selective channel into multiple narrow-band frequency flat channels for each subcarrier.

2. In OFDM, the orthogonality among sub-carriers is ensured, which improves bandwidth efficiency, spectral efficiency, and enables OFDMA.

3. OFDM can be seamlessly integrated with MIMO.

4. OFDM is based on Fast Fourier Transform (FFT) both at the transmitter and receiver. The FFT has lower complexity, can be easily scaled, and its implementation has a smaller silicon footprint while supporting hardware acceleration.

1.4 | Design of OFDM in 5G

The 5G uses three different implementations of CP-OFDM for PRACH, RIM-RS and rest of the channels. In the chapter, we will discuss the third one which is used by most of the physical channels. The implementation of CP-OFDM for PDSCH, PDCCH, PBCH, PUSCH, PUCCH and other chains in 5G is given by,

$$\bar{s_l}^{(p,\mu)}(t) = \sum_{k=0}^{N_{grid,x}^{\text{size},\mu}.N_{sc}^{RB}-1} a_{k,l}^{(p,\mu)} e^{j2\pi(k+k_0^{\mu}-N_{grid,x}^{\text{size},\mu}N_{sc}^{RB}/2).\Delta f.(t-N_{CP,l}^{\mu}T_c-t_{start,l}^{\mu})} \tag{1.16}$$

where

l : OFDM symbol index,
p : Antenna port index,
t : Time instant in time interval, $t^{\mu}_{\text{start},l} \leq t < t^{\mu}_{\text{start},l} + T^{\mu}_{\text{symb},l}$, of l-th OFDM symbol
μ : Numerology,
μ_0 : The largest μ value a UE is expected to support,
k : Subcarrier index,
k_0^{μ} : Subcarrier offset between the grids of numerology μ and μ_0,
$T^{\mu}_{\text{symb},l}$: Duration of l-th OFDM symbol $= (N^{\mu}_{\text{u}} + N^{\mu}_{\text{CP},l})T_c$
$N^{\mu}_{\text{CP},l}$: Cyclic prefix length for OFDM symbol-l with numerology (μ),
N^{μ}_{u} : FFT-size for numerology $(\mu) = 2048\kappa.2^{\mu}$,
T_c : Basic time unit for NR computed as $\dfrac{1}{\Delta f_{\max}.N_f}$ where $\Delta f_{\max} = 480 \times 10^3$ and $N_f = 4096$,
$N^{\text{size},\mu}_{grid,x}$: The size of resource grid. It represents the total bandwidth available at the BS.
N^{RB}_{sc} : Number of subcarriers per resource block. It is fixed to 12 in 5G,
$a^{(p,\mu)}_{k,l}$: Information loaded on subcarrier-k of antenna port (p) and numerology (μ) for OFDM symbol (l),
$\bar{s_l}^{(p,\mu)}(t)$: Time continuous signal on antenna port (p) and numerology (μ) for OFDM symbol (l).

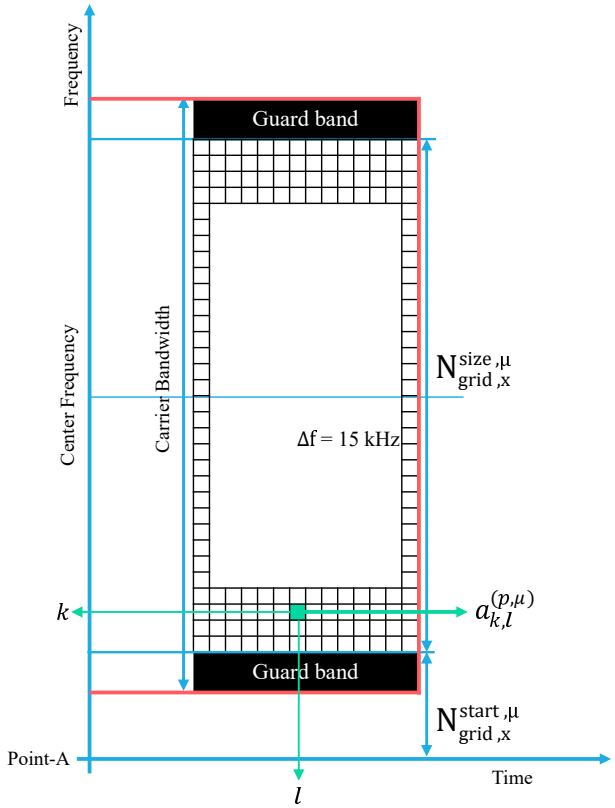

Figure 1.7: OFDM Resource Grid and Channel Bandwidth.

1.4.1 | Concept of Resource Grid

The 5G implementation of OFDM (Orthogonal Frequency Division Multiplexing) is based on the concept of the resource grid. A resource grid is a matrix or tensor that spans the complete bandwidth available at the base station across frequency and one slot (which typically consists of 14 OFDM symbols) across time,

as shown in Fig 1.7. The resource grid is organized into resource elements, which are Δf wide and span one OFDM symbol ($T^{\mu}_{\text{symb},l}$), capable of carrying one constellation symbol worth of information. The dimensions of the resource grid are $N_{\text{ports}} \times N_{\text{symb}} \times N_{\text{sc}}$, where the number of OFDM symbols and the number of sub-carriers in a resource grid are given by $N_{\text{symb}} = 142^{\mu}$ and $N_{\text{sc}} = 12N^{\text{size},\mu}_{grid,x}$, respectively. However, the BS can maintain the resource grid in units of 14 symbols as well, with separate resource grids for each numerology. Resources for data transmission, CSI-RS for channel sounding, sending control information, and broadcasting network information are allocated in the resource grid only.

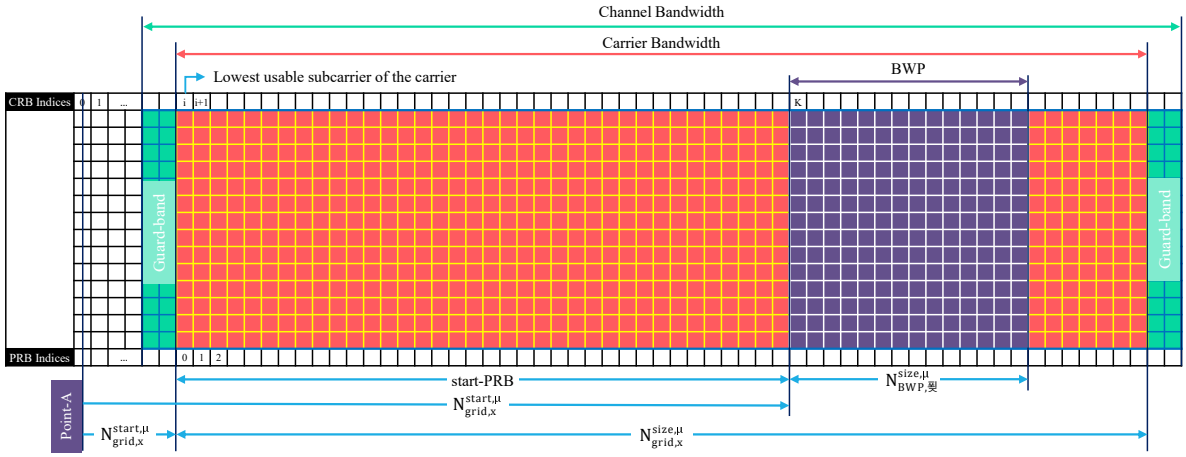

Figure 1.8: Channel Bandwidth, Carrier Bandwidth and BWP in 5G Networks.

1.4.2 | Numerologies in 5G Networks

The release 17 of 5G networks, unlike 4G networks, supports 7 numerologies/subcarrier spacing as shown in table 1.1. There numerologies allows the BS to find a judicious trade-off between receiver complexity, latency, cell coverage, robustness against CFO and Doppler.

Table 1.1: Numerologies in 5G

Numerology (μ)	Subcarrier spacing ($\Delta f = 15.2^{\mu}$) in kHz	Cyclic Prefix (CP) types
0	15	Normal
1	30	Normal
2	60	Normal and Extended
3	120	Normal
4	240	Normal
5	480	Normal
6	960	Normal

A subcarrier spacing of 240 kHz is reserved for the transmission of SSB, while other subcarrier spacings are employed for data transmission. Numerologies 0 and 1 (15/30 kHz) are used in FR1 (frequency range-sub 6 GHz). Numerology 2 (60 kHz) can be used in frequency ranges FR1 and FR2. Numerology 2 supports extended CP, which helps mitigate ISI under severe channel conditions. Numerology 3 and beyond are used in FR2, as FR2 is utilized in small cells with smaller propagation delay and delay spread, making them more suited for higher numerologies.

1.4.3 | Cyclic Prefix Length Selection in 5G Networks

The cyclic prefix length in 5G is not the same for all OFDM symbols. For 2 out of every $14 * 2^{\mu}$ symbols, a slightly longer cyclic prefix is used to ensure that the duration of a slot is $\frac{1}{2^{\mu}}$ milliseconds. Furthermore, with a 60 kHz subcarrier, the symbol duration reduces to 0.25 ms, and the cyclic prefix reduces proportionally, resulting in coverage of barely $180000/N_{\text{FFT}}$ meters, which is approximately 180

meters at a 200 MHz bandwidth. Hence, an extended cyclic prefix was introduced, as shown in equation 1.17. With the extended cyclic prefix, the coverage extends to 625 meters for a 60 kHz subcarrier spacing with a channel bandwidth of 200 MHz.

$$N^{\mu}_{\mathrm{CP},l} = \begin{cases} 512\kappa.2^{-\mu} & \text{extended CP (only applicable for } \Delta f = 60 \text{ kHz)} \\ 144\kappa.2^{-\mu} + 16\kappa & \text{normal CP, } l = 0 \text{ or } l = 7.2^{\mu} \\ 144\kappa.2^{-\mu} & \text{normal CP, } l \neq 0 \text{ and } l \neq 7.2^{\mu} \end{cases} \tag{1.17}$$

Furthermore, this variation in the length of CP for different symbols results in irregular OFDM symbol boundaries for the time (t) parameter stated in equation 1.16. The starting time instant for OFDM symbol-l is given by,

$$t^{\mu}_{\mathrm{start},l} = \begin{cases} 0 & l = 0 \\ t^{\mu}_{\mathrm{start},l-1} + T^{\mu}_{\mathrm{symb},l-1} & \text{otherwise} \end{cases} \tag{1.18}$$

1.5 | OFDM Implementation in 5G Toolkit

The implementation of OFDM consists of modulation at the transmitter and demodulation at the receiver. At the transmitter, the frequency resource grid is converted into time-domain OFDM samples before transmission across the air interface. Conversely, at the receiver, the time-domain samples are converted back into the frequency resource grid. In the subsection below, the detailed implementation of the OFDM transmitter and receiver is described. In 5G, the resources allocated for data transmission are within this resource grid.

1.5.1 | OFDM Implementation: Transmitter

The CP-OFDM modulation in the 5G Toolkit is implemented at the transmitter side using the class OFDMModulator. This module requires the length of the CP (L_{CP}) as a parameter. The OFDM modulation of the input resource grid is performed, which is expected to be either a 1D or 2D matrix or a tensor. The modulation is carried out across the last dimension of the resource grid, and the size of the last dimension is considered as the FFT size. The frequency domain grid of shape 14 (number of OFDM symbols) $\times$ N_{FFT} is passed on to the object of the class, which generates the time-domain OFDM samples at the output of size ($N_{\mathrm{FFT}} + L_{\mathrm{CP}}$) $\times$ number of OFDM symbols.

Note: The OFDM modulator attaches the same length CP to all OFDM symbols. To conform to 3GPP standards, we pass the grid symbol by symbol to the OFDM modulator, where the length of the CP attached to each symbol is computed using the **lengthCP** variable returned by the TimeFrequency5GParameters class in the 5G Toolkit.

1.5.2 | OFDM Implementation: Receiver

The received time-domain samples are passed to the OFDM demodulator defined in the 5G Toolkit by OFDMDemodulator. This module removes the L_{CP} samples, assuming them as the cyclic prefix, and reconstructs the OFDM resource grid. The module expects two parameters as inputs

- FFT-size (N_{FFT}) and,
- length of CP (L_{CP})

to reconstruct the resource grid of size $(\ldots, N_{\mathrm{symb}}, N_{\mathrm{FFT}})$ from the received time-domain samples of shape $(\ldots, N_{\mathrm{symb}}.(N_{\mathrm{FFT}} + L_{\mathrm{CP}}) + n)$, where n is a non-negative number.

1.6 | Results

In this section, we will demonstrate the effect of the OFDM and system parameters on the behavior of the resource grid, frequency selectivity, and a few hardware impairments such as CFO. The observations will be made based on the parameters stated in table 1.2.

Table 1.2: Simulation Parameters for OFDM evaluations

Parameters	Value
Center frequency (f_c)	1000 MHz
Bandwidth (B)	5 MHz
FFT-size (N_{FFT})	2048/1024/512/256
Subcarrier spacing (Δf)	15/30/60/120 kHz
Transmitter-receiver separation	1 m

Observation-1: The time and frequency location of the information in transmitted and received OFDM resource grid are exactly the same if the systems are accurately synchronized.

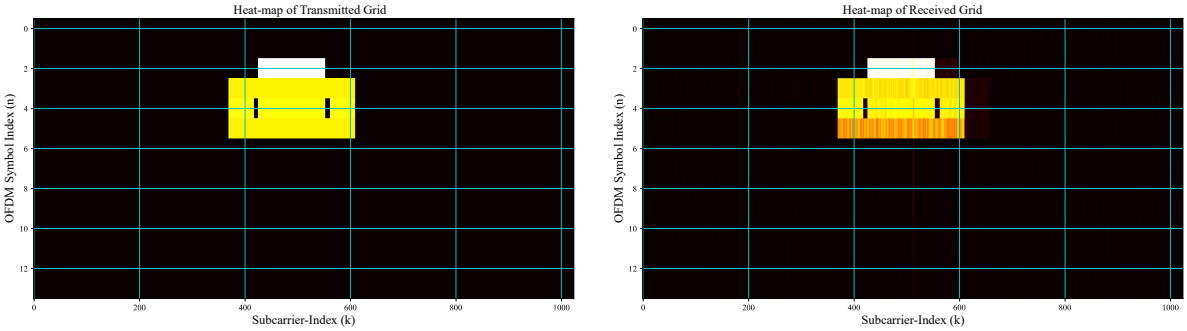

(a) Heat-map of transmitted resource grid **(b)** Heat-map of received resource grid

Figure 1.9: Comparison between the tx and rx resource grid for $N_{\text{FFT}} = 1024$ and $\Delta f = 15$ KHz

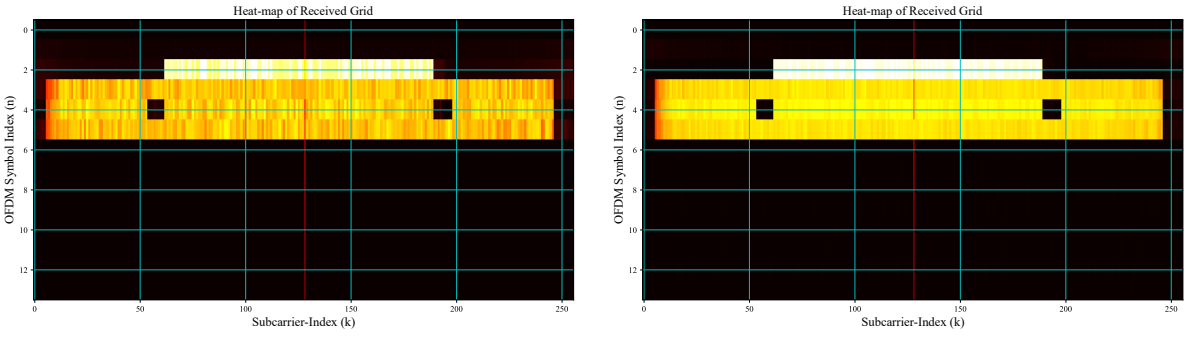

(a) $\Delta f = 15$ kHz and N_{FFT} =256 **(b)** $\Delta f = 30$ kHz and N_{FFT} =256

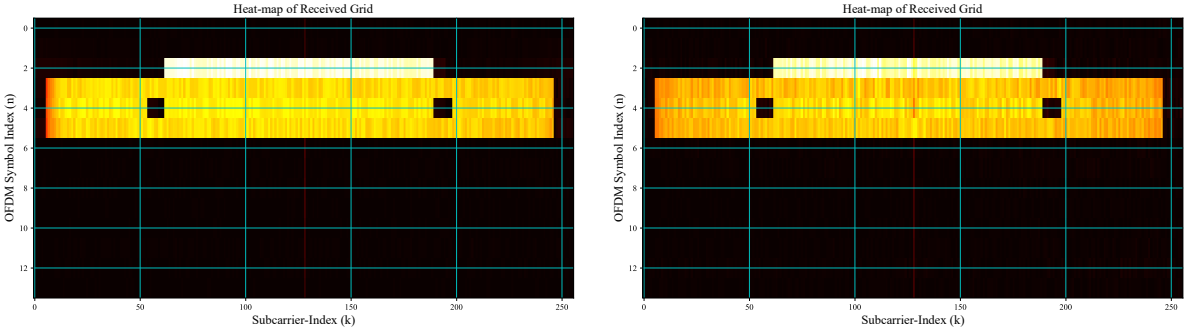

(c) $\Delta f = 60$ kHz and N_{FFT} =256 **(d)** $\Delta f = 120$ kHz and N_{FFT} =256

Figure 1.10: Analysis of quality of received grid for different subcarrier spacing for fixed FFT size.

The heat-map of power distribution in the resource grid transmitted and received by the SDR is shown in Fig 1.9. It can be seen that if the SDR receiver synchronizes in time accurately and mitigates the CFO and Doppler offset to a low enough level, the resource grids can be reconstructed pretty accurately owing

to the orthogonality between the subcarrier tones. The red lines in figure 1.9b shows distortions in the received grid due to DC offset, residual frequency offsets, and thermal noise.

Observation-2: The impact of residual frequency offsets is lower on higher subcarrier spacing for a fixed FFT-size.

The effect of the residual frequency offset is directly proportional to $\frac{f_{\text{RFO}}}{\Delta f}$. It can be observed from the equation that higher is the subcarrier spacing lower is the effect of the residual frequency offsets on the performance of OFDM. The same inferences can be drawn from the results shown in Fig-1.10 where SDR based emulations are performed for different subcarrier spacing Δf for a fixed FFT-size.

Observation-3: The impact of residual frequency offsets is lower on OFDM system using higher sample rates for a fixed subcarrier spacing.

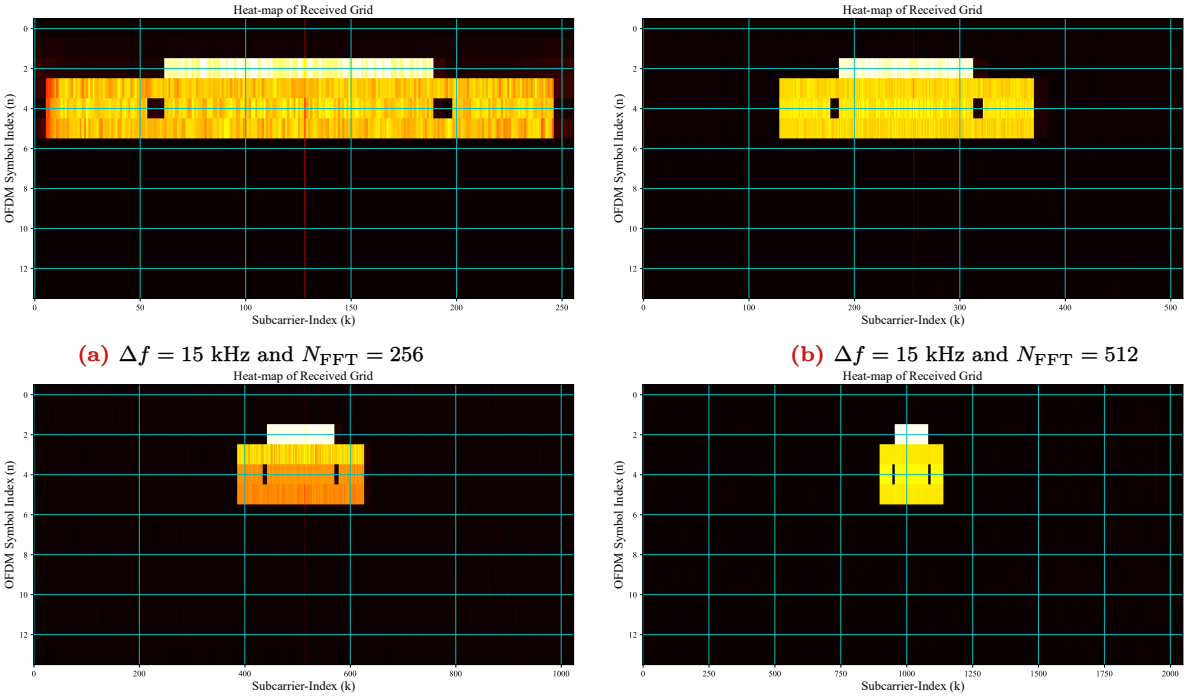

(a) $\Delta f = 15$ kHz and $N_{\text{FFT}} = 256$

(b) $\Delta f = 15$ kHz and $N_{\text{FFT}} = 512$

(c) $\Delta f = 15$ kHz and $N_{\text{FFT}} = 1024$

(d) $\Delta f = 15$ kHz and $N_{\text{FFT}} = 2048$

Figure 1.11: Analysis of quality of received resource grid for different FFT-size for a fixed $\Delta f = 15$ kHz.

It is clearly observed from the above figures that there is no significant effect of subcarrier spacing on reception of SSB. However, for subcarrier spacing of 15 KHz, the fading is a little higher.

1.7 | Useful Resources

The following are some good references to understand OFDM and OFDM in 5G Networks. You can find the link to the codes used in this tutorial.

- OFDM Documentation in 5G Toolkit.
- A Tutorial in 5G Networks.
- Detailed Python Code of this Experiment.
- A Video Tutorial for this Experiment.
- Details of OFDM implementation in 5G networks [1].

2 | References

[1] TS 38.211 3rd Generation Partnership Project. Physical channels and modulation (Release 17). *Technical Specification Group Radio Access Network*, Version(v17.5.0):35–52, 2023-06.

[2] Douglas H Morais. *Key 5G physical layer technologies*. Springer, 2020.